

Performance of the turbo coded HomePlug AV system over power-line channels

L. Guerrieri, P. Bisaglia, G. Dell'Amico, E. Guerrini

Dora Spa, STMicroelectronics Group, Via Laboratori Vittime del Col du Mont 24, 11100 Aosta, Italy

Email: lorenzo-dora-spa.guerrieri@st.com

Abstract—The next generation technology of HomePlug, called HomePlug AV, aims at providing very high-quality connectivity for the in-home distribution of data and multi-stream entertainment using existing power-line wiring. To obtain very robust performance a powerful turbo convolutional code is adopted.

In this paper, by means of simulations, the performance of the turbo coded HomePlug AV system is examined under a realistic power-line channel model. In particular, the effects of the interleaver's length and of the number of iterations in an improved Max-Log-MAP turbo decoder are investigated. Results show that few iterations of the turbo decoding process give a massive gain in performance under the considered environment.

Keywords—Turbo coding, interleaver, OFDM, HomePlug AV.

I. INTRODUCTION

IN the last few years, the development of home networks, providing multiple PCs with access to shared resources such as printers, scanners and Internet connection, has received a great deal of attention. Besides the traditional Ethernet-based design, alternative solutions have been deployed ranging from wireless to power-lines or phone-lines, requiring no installation of new cables, central hubs or switches, and hence making them easier to install and use. Power line networks, operating across the same wires and outlets as electrical appliances, appear to be very attractive for their greater ubiquity with respect to phone-lines, and greater quality of service (QoS) and house coverage with respect to wireless solutions.

To this end, HomePlug, an industrial organization that comprises more than 70 companies, was formed in 2000 to develop and standardize specifications for home networking technology using existing power-line wiring. The first release of HomePlug in June 2001, called HomePlug 1.0, was followed in July 2005 by a second release, called HomePlug AV [1].

The HomePlug AV system, supporting raw data rates up to 150 Mbit/s, employs adaptive orthogonal frequency division multiplexing (OFDM) over a bandwidth from 1.8 to 30 MHz, using 917 useful sub-carriers. The possible modulations, employed per sub-carrier, range from a BPSK to a 1024-QAM. Robust performance is obtained through the use of a turbo convolutional code, which should cope with the frequency selective and noisy channels, that characterize in-home power-line transmissions [2]. Indeed, since their appearance in 1993 [3], turbo codes have found many applications in different fields [4], [5]. In [6], [7] an extensive overview of the HomePlug AV is given. However, to our knowledge, no previous results have been published evaluating the performance of the turbo coded HomePlug AV system under a realistic environment.

In this paper an improved Max-Log-MAP turbo decoder [8] for the HomePlug AV system is proposed and its performance over an AWGN and power-line channels presented, and compared also with the conventional Max-Log-MAP [9] and MAP [10] turbo decoders. In particular, the effects of the interleaver's length and of the number of iterations in the improved Max-Log-MAP turbo-decoder are investigated. We note that, recently in [11], a turbo coded HomePlug-like system was considered; unfortunately, the results presented in [11] refer to a completely different OFDM setting, and a direct derivative of the turbo coded HomePlug AV system performance appears to be difficult.

The paper is organized as follows: in Section II the physical layer of the HomePlug AV system is reviewed, while details on the implemented soft-input soft-output (SISO) de-mapper and the turbo decoder are illustrated in Sections III and IV; numerical results are reported in Section V with conclusions given in Section VI.

II. SYSTEM MODEL

In Figure 1 the HomePlug AV (HPAV) physical layer [1], [6] on which we base our analysis is shown¹. At the transmitter, the information bits for HPAV data transmission, after scrambling, are turbo convolutionally encoded, with rate 1/2, bit-by-bit interleaved and then converted into QAM symbols through a bit-mapper. The data symbols (belonging to unit power constellations) are serial-to-parallel-converted for OFDM modulation. Each OFDM sub-carrier can be differently loaded, depending on the estimated SNR per sub-carrier, with one of the following modulations: BPSK, 4-QAM, 8-QAM, 16-QAM, 64-QAM, 256-QAM and 1024-QAM. In HPAV the OFDM modulation is implemented by using a 3072-point inverse discrete Fourier transform (IDFT). Furthermore, to comply with frequency regulatory bodies, only 917 sub-carriers, out of the 1536 sub-carriers from DC to 37.5 MHz, are employed for useful transmission. To reduce the complexity of the receiver, a suitable cyclic prefix is used to remove both inter-symbol and inter-channel interference (ISI and ICI). Finally, before an analog front end (AFE) block, which sends the resulting signal to the power-line channel, a peak limiter block is inserted to minimize the peak-to-average power ratio (PAPR).

¹As explained in [6] the input bits from the MAC are structured by the HPAV transmitter differently depending on whether they are HPAV data, HPAV control information or HomePlug 1.0 control information. In this paper, for the sake of simplicity, we will refer to the more common HPAV formats only.

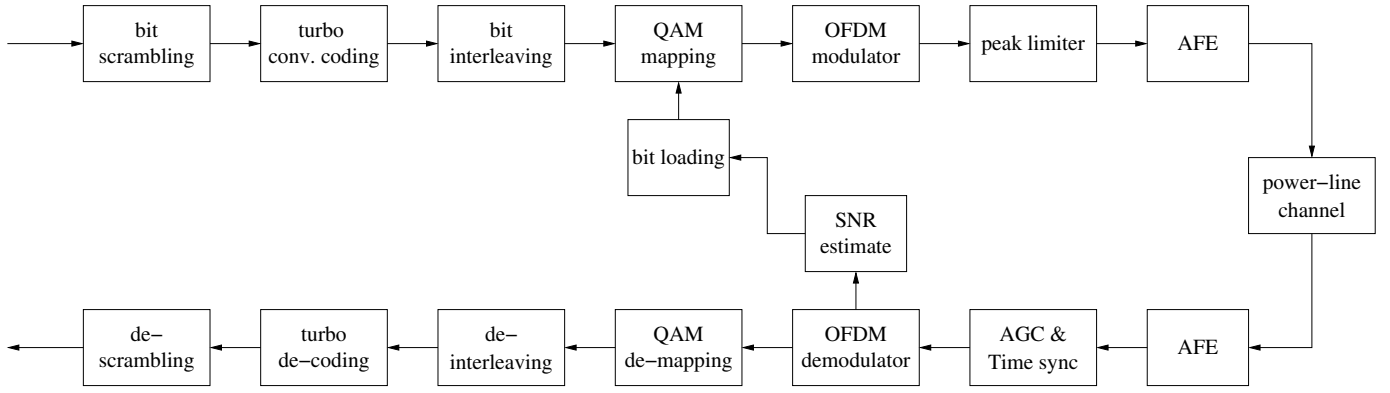


Fig. 1. Block diagram of the HomePlug AV physical layer, for data transmission.

At the receiver the signal after the AFE block is fed to an automatic gain control (AGC) and time synchronism blocks. In this paper both blocks will be assumed to be ideal. After cyclic prefix removal and OFDM demodulation, which is implemented by the 3072-point discrete Fourier transform (DFT), and assuming the following: that the cyclic prefix completely eliminates ISI and ICI; that we can guarantee perfect synchronization; and that the channel is time invariant within each i -th OFDM symbol, the received signal over the generic sub-carrier k , for $k = 0, \dots, N - 1$, can be written as:

$$y_i[k] = G_i[k]a_i[k] + n_i[k] \quad (1)$$

$a_i[k]$, $G_i[k]$ and $n_i[k]$ denote the transmitted QAM symbol, the channel frequency response complex coefficient and the complex additive noise with variance $\sigma_i^2[k]$, over the generic k -th sub-carrier during the i -th OFDM symbol, respectively.

The output from the OFDM demodulator is then sent to a SISO de-mapper, a de-interleaver, a turbo convolutional decoder and a de-scrambler to reconstruct and estimate the transmitted bits.

In the following two sections details on how the SISO de-mapper and the turbo convolutional decoder have been implemented will be given.

III. SISO DE-MAPPER

Let $M = 2^m$ be the number of symbols $\{\alpha = \alpha_I + j\alpha_Q\}$ of the generic HomePlug AV constellation \mathcal{A} , so that m interleaved coded bits (of values 0 and 1) are mapped into the complex symbol. Let $a_i[k] = a_{I,i}[k] + ja_{Q,i}[k]$ denote the symbol transmitted over the generic k -th sub-carrier during the i -th OFDM symbol and $\{c_{i_1}[k], \dots, c_{i_m}[k]\}$ the corresponding coded bit sequence. For each bit $c_{i_l}[k]$ the constellation is split into two partitions of complex symbols, namely $S_{i_l}^{(0)}$, comprising the coded bits with a '0' in position i_l , and $S_{i_l}^{(1)}$ the complementary partition. Let introduce the notations

$$z_i[k] = y_i[k]/G_i[k] \quad (2)$$

and

$$D_{i_l}[k] = \frac{1}{4} \left(\min_{\alpha \in S_{i_l}^{(0)}} |z_i[k] - \alpha|^2 - \min_{\alpha \in S_{i_l}^{(1)}} |z_i[k] - \alpha|^2 \right) \quad (3)$$

The log-likelihood ratio (LLR) of the decision bit $\hat{c}_{i_l}[k]$ from the de-mapper, can be approximated by [12]

$$\lambda_{i_l}[k] = \ln \left(\frac{P[c_{i_l}[k] = 1|y_i[k]]}{P[c_{i_l}[k] = 0|y_i[k]]} \right) \approx \frac{2|G_i[k]|^2}{\sigma_i^2[k]} \cdot D_{i_l}[k] \quad (4)$$

In the following two sections we will derive further simplified expressions for all the square QAM constellations of HomePlug AV, while report the expression of $D_{i_l}[k]$ in the case of the 8-QAM constellation (the only not-square constellation of the system).

A. Square QAM constellations

For square QAM constellations m is even, hence $m/2$ interleaved coded bits (of values 0 and 1) are mapped into the in-phase (real, \Re) and quadrature (imaginary, \Im) components of the complex symbol. Let now rename the bit sequence, corresponding to the $a_i[k]$ QAM symbol, as $\{c_{I,i_1}[k], \dots, c_{I,i_{m/2}}[k], c_{Q,i_1}[k], \dots, c_{Q,i_{m/2}}[k]\}$, and let introduce the notations

$$z_{I,i}[k] = \Re\{y_i[k]/G_i[k]\} \quad (5)$$

and

$$D_{I,i_l}[k] = \frac{1}{4} \left(\min_{\alpha_I \in S_{I,i_l}^{(0)}} (z_{I,i}[k] - \alpha_I)^2 - \min_{\alpha_I \in S_{I,i_l}^{(1)}} (z_{I,i}[k] - \alpha_I)^2 \right) \quad (6)$$

where $S_{I,i_l}^{(c)} \triangleq \Re\{S_{i_l}^{(c)}\}$ contains the real parts of the complex symbols of subset $S_{i_l}^{(c)}$, for $c = 0, 1$ and $l = 1, \dots, m/2$. The LLR of the decision bit $\hat{c}_{I,i_l}[k]$ from the de-mapper, can now be approximated as

$$\lambda_{I,i_l}[k] = \ln \left(\frac{P[c_{I,i_l}[k] = 1|y_i[k]]}{P[c_{I,i_l}[k] = 0|y_i[k]]} \right) \approx \frac{2|G_i[k]|^2}{\sigma_i^2[k]} \cdot D_{I,i_l}[k] \quad (7)$$

A similar derivation holds true for bits $\hat{c}_{Q,i_l}[k]$, starting from $z_{Q,i}[k] = \Im\{y_i[k]/G_i[k]\}$. The main simplification of (7) with respect to (4), as explained in [12], lies in the fact that the two-dimensional Euclidean distances from M constellation points of (3) reduce to one-dimensional Euclidean distances from \sqrt{M} points of (6), allowing to significantly decrease the computational complexity. Further simplified expressions of

$D_{I,i}[k]$ for $M = 16$ and 64 can be found in [12]²; in the following we report simplified expressions also for $M = 256$ and 1024 , based on the same criterion of [12].

The approximated expressions for the four in-phase bits of a 256-QAM constellation are given by:

$$\begin{aligned}
D_{I,i_1}[k] &= - \left| - \left| \frac{|z_{I,i}[k]|}{\sqrt{170}} - \frac{8}{170} \right| + \frac{4}{170} \right| + \frac{2}{170} \\
D_{I,i_2}[k] &\approx - \frac{\left| |z_{I,i}[k]| - \frac{8}{\sqrt{170}} \right| - \frac{4}{\sqrt{170}}}{4} \\
&\quad \left(\frac{2}{\sqrt{170}} + \left| \left| |z_{I,i}[k]| - \frac{8}{\sqrt{170}} \right| - \frac{4}{\sqrt{170}} \right| \right) \\
D_{I,i_3}[k] &\approx \frac{|z_{I,i}[k]| - \frac{8}{\sqrt{170}}}{4} \left(\frac{2}{\sqrt{170}} + \left| |z_{I,i}[k]| - \frac{8}{\sqrt{170}} \right| \right) \\
D_{I,i_4}[k] &\approx \frac{z_{I,i}[k]}{4} \left(\frac{2}{\sqrt{170}} + |z_{I,i}[k]| \right) \quad (8)
\end{aligned}$$

It can be easily verified that the $D_{Q,i}[k]$ functions for the four quadrature bits are the same as in (8) with $z_{I,i}[k]$ replaced by $z_{Q,i}[k]$. We note that, comparing the expressions in (8) with the ones derived in [12], normalization factors appear. This is because HomePlug AV imposes unit power constraints. For the 1024-QAM constellation the approximated expressions for the five in-phase bits are:

$$\begin{aligned}
D_{I,i_1}[k] &= - \left| - \left| \frac{|z_{I,i}[k]|}{\sqrt{682}} - \frac{16}{682} \right| + \frac{8}{682} \right| + \frac{4}{682} + \frac{2}{682} \\
D_{I,i_2}[k] &\approx - \frac{\left| \left| |z_{I,i}[k]| - \frac{16}{\sqrt{682}} \right| - \frac{8}{\sqrt{682}} \right| - \frac{4}{\sqrt{682}}}{4} \\
&\quad \left(\frac{2}{\sqrt{682}} + \left| \left| |z_{I,i}[k]| - \frac{16}{\sqrt{682}} \right| - \frac{8}{\sqrt{682}} \right| - \frac{4}{\sqrt{682}} \right) \\
D_{I,i_3}[k] &\approx - \frac{\left| |z_{I,i}[k]| - \frac{16}{\sqrt{682}} \right| - \frac{8}{\sqrt{682}}}{4} \\
&\quad \left(\frac{2}{\sqrt{682}} + \left| \left| |z_{I,i}[k]| - \frac{16}{\sqrt{682}} \right| - \frac{8}{\sqrt{682}} \right| \right) \\
D_{I,i_4}[k] &\approx \frac{|z_{I,i}[k]| - \frac{16}{\sqrt{682}}}{4} \left(\frac{2}{\sqrt{682}} + \left| |z_{I,i}[k]| - \frac{16}{\sqrt{682}} \right| \right) \\
D_{I,i_5}[k] &\approx \frac{z_{I,i}[k]}{4} \left(\frac{2}{\sqrt{682}} + |z_{I,i}[k]| \right) \quad (9)
\end{aligned}$$

We observe that expressions (8) and (9) in some cases exhibit a parabolic behavior, differently from the linear behavior given in (24) of [12]. This has been done to better approximate for high-density constellations all the LLRs to be used in the turbo decoding process.

²We highlight that minor changes are required in the expressions of [12] to fulfil the different Gray patterns and power constraints in the HomePlug AV constellations compared to those of HIPERLAN/2.

B. 8-QAM constellation

Finally, for the HomePlug AV 8-QAM constellations the three LLR expressions are:

$$\begin{aligned}
D_{I,i_1}[k] &= \frac{|z_{I,i}[k]|}{\sqrt{5 + 1.29^2}} - \frac{2}{5 + 1.29^2} \\
D_{I,i_2}[k] &\approx \frac{z_{I,i}[k]}{\sqrt{5 + 1.29^2}} \\
D_{Q,i_1}[k] &= \frac{1.29 z_{Q,i}[k]}{\sqrt{5 + 1.29^2}} \quad (10)
\end{aligned}$$

IV. TURBO DECODER

The turbo decoder scheme we have implemented is depicted in Figure 2 and here only briefly illustrated³. The first SISO decoder elaborates the systematic part λ_t^s and the first parity part λ_t^p of the channel de-interleaved LLR from the SISO de-mapper (see previous section) together with the a priori probability $\Lambda_{t,ext}^{2 \rightarrow 1}$ to give the extrinsic information $\Lambda_{t,ext}^{1 \rightarrow 2}$. The second SISO decoder processes the turbo interleaved systematic part λ_z^s , the second parity part λ_z^p of the channel de-interleaved LLR from the SISO de-mapper and the a priori probability $\Lambda_{z,ext}^{1 \rightarrow 2}$ which results from the turbo interleaver. The output from the SISO decoder 2, i.e. the extrinsic information $\Lambda_{z,ext}^{2 \rightarrow 1}$ is turbo de-interleaved and the algorithm is iterated. After a suitable number of iterations the a posteriori probability Λ_t^q is passed to the hard decision unit for the final decision. We note that the iterative feature of the algorithm allows to make use of a single SISO decoder module which alternately works as decoder 1 or decoder 2 in the hardware implementation. In our realization the SISO module can implement the Bahl, Cocke, Jelinek and Raviv (BCJR) algorithm in three different forms: i) optimum maximum a posteriori probability (MAP), ii) sub-optimum Max-Log-MAP and iii) improved Max-Log-MAP. We sketch here only a brief description of them. The interested reader should refer to [8], [9], [10] for a more detailed description of the algorithms.

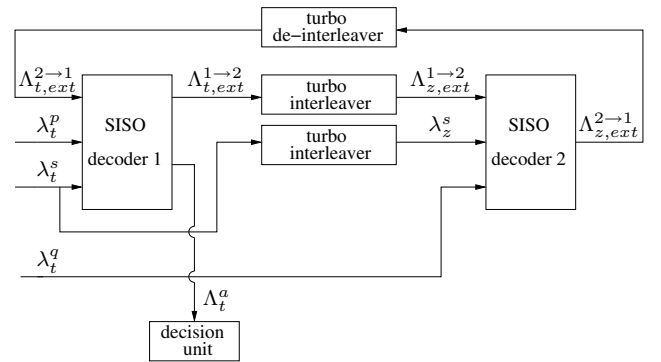


Fig. 2. Block diagram of the iterative turbo decoder.

³In the following expressions, t and z index the decoder inputs while the OFDM sub-carrier and symbol indices have been dropped.

A. Maximum a posteriori probability (MAP)

The MAP algorithm [10] bases its decision on the a posteriori probability Λ_t^a given by:

$$\Lambda_t^a(u_n, u_m) = \ln \left(\frac{\sum_{S_i \xrightarrow{u_n} S_j} \alpha_{t-1}(i) \gamma_t(i, j) \beta_t(j)}{\sum_{S_i \xrightarrow{u_m} S_j} \alpha_{t-1}(i) \gamma_t(i, j) \beta_t(j)} \right) \quad i, j \in \mathbb{N}_s \quad (11)$$

where $\mathbb{N}_s = \{1, 2, \dots, s\}$, with s denoting the encoder state number, and the numerator and the denominator sums are made over all the possible state transitions $S_i \rightarrow S_j$ caused by the encoder inputs u_n and u_m , respectively. The time dependent s -dimensional vector α_t , called *forward (past) metric*, and the s -dimensional vector β_t , called *backward (future) metric*, are derived recursively by the following equations:

$$\begin{cases} \alpha_0(S_{\text{start}}) = 1, & \alpha_0(S_i) = 0 \quad \forall S_i \neq S_{\text{start}} \\ \alpha_t = \alpha_{t-1} \gamma_t & \forall t \in \mathbb{N}_L \end{cases} \quad (12)$$

$$\begin{cases} \beta_L(S_{\text{end}}) = 1, & \beta_L(S_i) = 0 \quad \forall S_i \neq S_{\text{end}} \\ \beta_t = \gamma_{t+1} \beta_{t+1} & \forall t \in \mathbb{N}_{L-1} \end{cases} \quad (13)$$

In the above equations L is the HomePlug AV turbo interleaver length⁴, $\mathbb{N}_L = \{1, 2, \dots, L\}$, S_{start} and S_{end} denote the initial and the final encoder states, respectively, and γ_t is the time dependent $s \times s$ *state (present) matrix*, whose elements are given by:

$$\gamma_t(i, j) = P[S_t = j, \lambda_t | S_{t-1} = i] \quad \forall t \in \mathbb{N}_L \quad (14)$$

where $\lambda_t = [\lambda_t^s, \lambda_t^p]$. In (14), the systematic (intrinsic) and the a priori (extrinsic) terms can be factored out and (11) becomes

$$\Lambda_t^a(u_n, u_m) = \Lambda_{t, \text{int}}(u_n, u_m) + \Lambda_{t, \text{ext}}^{2 \rightarrow 1}(u_n, u_m) + \Lambda_{t, \text{ext}}^{1 \rightarrow 2}(u_n, u_m) \quad (15)$$

where $\Lambda_{t, \text{int}}(u_n, u_m)$ is the intrinsic LLR and $\Lambda_{t, \text{ext}}^{1 \rightarrow 2}(u_n, u_m)$ is given by:

$$\Lambda_{t, \text{ext}}^{1 \rightarrow 2}(u_n, u_m) = \ln \left(\frac{\sum_{S_i \xrightarrow{u_n} S_j} \alpha_{t-1}(i) \gamma_{t, \text{ext}}(i, j) \beta_t(j)}{\sum_{S_i \xrightarrow{u_m} S_j} \alpha_{t-1}(i) \gamma_{t, \text{ext}}(i, j) \beta_t(j)} \right) \quad i, j \in \mathbb{N}_s \quad (16)$$

B. Max-Log-MAP

It is well-known that the MAP algorithm is computationally cumbersome due to the non-linear operations involved in its derivation. To cope with this problem the simpler Max-Log-MAP algorithm has followed [9]. This is based on the following approximation:

$$\sum_k \exp(w_k) \approx \exp(\max_k(w_k)) \quad (17)$$

⁴The HomePlug AV system allows three possible interleavers, that we will denote as interleaver 1 (of length 64), interleaver 2 (of length 544) and interleaver 3 (of length 2080) in the numerical results section.

By defining $\Gamma_t = \ln(\gamma_t)$, $\mathbf{A}_t = \ln(\alpha_t)$, $\mathbf{B}_t = \ln(\beta_t)$ and inserting (17) in (12), (13), (15) and (16) we obtain

$$A_t(i) \approx \max_{l \in \mathbb{N}_s} (A_{t-1}(l) + \Gamma_t(l, i)) \quad \forall i \in \mathbb{N}_s, \forall t \in \mathbb{N}_L \quad (18)$$

$$B_t(i) \approx \max_{l \in \mathbb{N}_s} (B_{t+1}(l) + \Gamma_{t+1}(i, l)) \quad \forall i \in \mathbb{N}_s, \forall t \in \mathbb{N}_{L-1} \quad (19)$$

$$\Lambda_t^a(u_n, u_m) \approx \Lambda_{t, \text{int}}(u_n, u_m) + \Lambda_{t, \text{ext}}^{2 \rightarrow 1}(u_n, u_m) + \Lambda_{t, \text{ext}}^{1 \rightarrow 2}(u_n, u_m) \quad (20)$$

$$\Lambda_{t, \text{ext}}^{1 \rightarrow 2}(u_n, u_m) \approx \max_{S_i \xrightarrow{u_n} S_j} (A_{t-1}(i) + \Gamma_{t, \text{ext}}(i, j) + B_t(j)) - \max_{S_i \xrightarrow{u_m} S_j} (A_{t-1}(i) + \Gamma_{t, \text{ext}}(i, j) + B_t(j)) \quad (21)$$

C. Improved Max-Log-MAP

Finally, following the suggestion of Vogt and Finger [8], the improved Max-Log-MAP algorithm is simply obtained from the classical Max-Log-MAP algorithm by multiplying the extrinsic information by a factor δ :

$$\Lambda_{t, \text{ext}}^{1 \rightarrow 2}(u_n, u_m) \approx \delta \left(\max_{S_i \xrightarrow{u_n} S_j} (A_{t-1}(i) + \Gamma_{t, \text{ext}}(i, j) + B_t(j)) - \max_{S_i \xrightarrow{u_m} S_j} (A_{t-1}(i) + \Gamma_{t, \text{ext}}(i, j) + B_t(j)) \right) \quad (22)$$

V. NUMERICAL RESULTS

A. AWGN channel

In order to evaluate the potential of the iterative turbo decoder of HomePlug AV, we first consider an additive white Gaussian noise channel (AWGN), and assume perfect signal-to-noise ratio (SNR) and timing knowledge. The results, obtained by computer simulations, are given in terms of the average bit error rate (BER) as a function of the received SNR.

In Figure 3 we compare the performance of the Max-Log-MAP and the improved Max-Log-MAP decoders, for BPSK

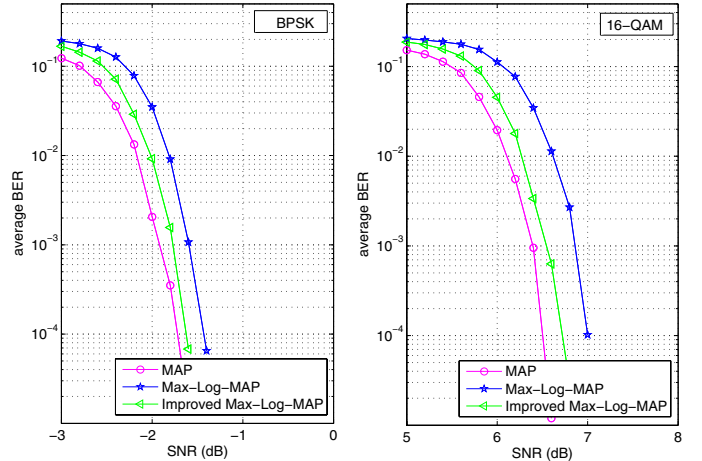


Fig. 3. BER versus SNR over an AWGN channel: BPSK on the left and 16-QAM on the right. Comparison between MAP, Max-Log-MAP and improved Max-Log-MAP decoders with the turbo interleaver 2 and 10 iterations.

(on the left) and 16-QAM (on the right) modulations⁵, using the turbo interleaver 2 (the intermediate interleaver’s length of the HomePlug AV). For the improved Max-Log-MAP, the scaling factor δ giving the best performance was chosen⁶. As an optimal lower-bound, we also report the performance of the MAP decoder. All the decoders are compared for the same number of iterations equal to 10. As it can be observed, the improved Max-Log-MAP decoder, for a small increase in computational complexity with respect to the Max-Log-MAP decoder, gives, for both depicted constellations, performance very close to the MAP’s bound. For instance, at a BER = 10^{-3} the degradation in performance of the improved Max-Log-MAP decoder with respect to the MAP decoder is of 0.1 dB for the BPSK and the 16-QAM modulations. Moreover, the improved Max-Log-MAP decoder gives 0.2 dB performance gain compared to the standard Max-Log-MAP decoder for the BPSK modulation, and 0.3 dB for the 16-QAM modulation. Furthermore, results, not reported here, have shown that analogous relative performance between the different algorithms is maintained as the constellation, the number of iterations or the interleaver’s length is changed. For this reason, due to its good tradeoff between performance and computational complexity, the improved Max-Log-MAP decoder will be used in all the following simulation results.

Results, by varying the number of iterations, for the improved Max-Log-MAP turbo decoder with the turbo interleaver 2 are depicted in Figure 4, for BPSK (on the left) and 16-QAM (on the right) modulations. For the BPSK modulation at a BER = 10^{-3} , the turbo decoding gain, compared to the first iteration⁷, is equal to 2.6 dB after the second iteration, 3.3 dB after the third, 3.5 dB after the fourth, 3.6 dB after the

⁵We highlight that the HomePlug AV system allows allocating different modulations over the different sub-carriers (bit-loading). In this paper, however, in order to see the performance of the turbo code on the single modulations, we will keep the same modulation fixed over all the sub-carriers.

⁶As observed in [8] the best scaling factor lies between 0.7 and 1.

⁷By first iteration we mean the output from the decision unit block in Figure 2 after the SISO decoder 1 has decoded the information once.

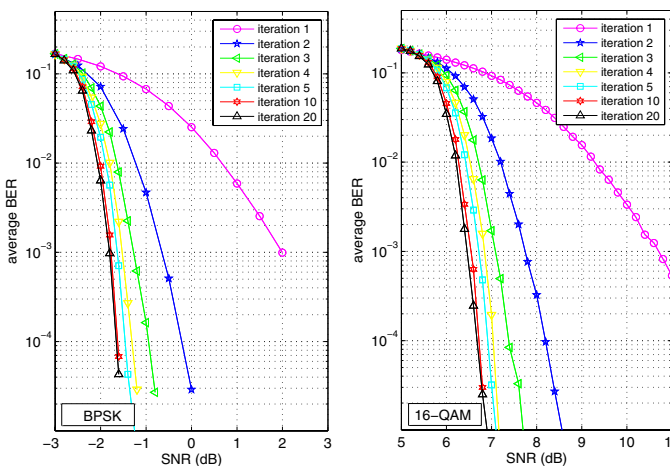


Fig. 4. BER versus SNR over an AWGN channel: BPSK on the left and 16-QAM on the right. Performance of the improved Max-Log-MAP decoder with the turbo interleaver 2, at different iteration numbers.

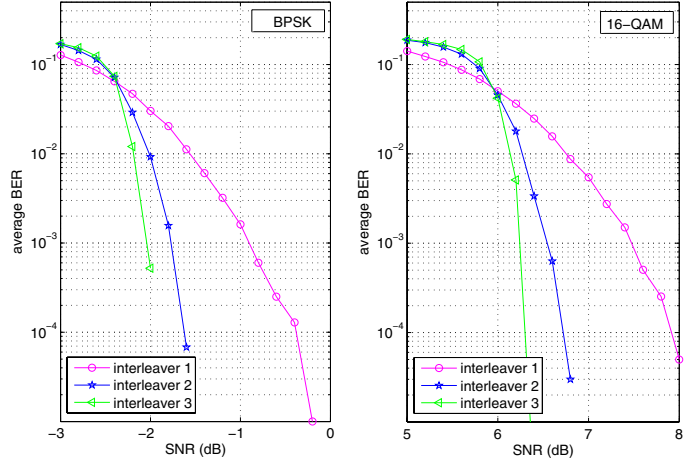


Fig. 5. BER versus SNR over an AWGN channel: BPSK on the left and 16-QAM on the right. Performance of the improved Max-Log-MAP decoder with different turbo interleavers and 10 iterations.

fifth, and 3.8 dB after the tenth iteration. Further iterations achieve only a marginal gain. After the twentieth iteration the total gain with respect to the first iteration is almost the same as after the tenth iteration and 8.6 dB compared to an un-coded HomePlug AV system⁸ (curve not reported in the figure). A similar trend is observed for the 16-QAM modulation—where the total gain with respect to the un-coded system is almost 10 dB, after the twentieth iteration—and all the other modulations (although results have not been included).

As a last comparison over an AWGN channel, Figure 5 depicts the performance of the improved Max-Log-MAP turbo decoder with 10 iterations by varying the turbo interleaver’s length, for BPSK (on the left) and 16-QAM (on the right) modulations. As it can be noticed, the longest turbo interleavers, namely interleaver 2 and 3, at the expense of a greater latency, provide a big improvement with respect to interleaver 1 (the shortest interleaver’s length of the HomePlug AV). In particular, at a BER = 10^{-3} the gain of the turbo interleaver 2 with respect to interleaver 1 is of 0.9 dB; in turn, the interleaver 3 allows a further gain of roughly 0.3 dB over the interleaver 2. A similar trend is observed for the 16-QAM modulation and all the other modulations (although results have not been included).

B. Power-line channel

Figures 6 and 7 show results in a typical power-line scenario. As in [13], a multi-path channel is assumed; furthermore, according to [14], [15], two kinds of noise are also considered: additive colored Gaussian noise and narrow-band interference. The results, obtained by computer simulations, are given in terms of the average BER as a function of the average received SNR, assuming perfect SNR and timing knowledge.

⁸Although the system does not include the un-coded option, nonetheless here we also consider this case.

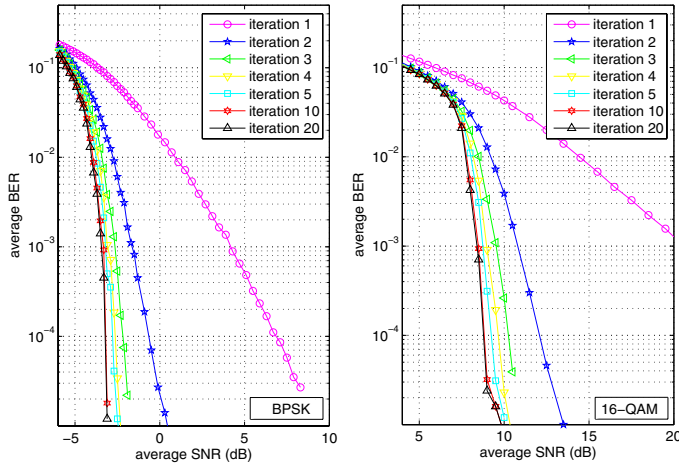


Fig. 6. Average BER versus average SNR, over a power-line channel: BPSK on the left and 16-QAM on the right. Performance of the improved Max-Log-MAP decoder with the turbo interleaver 2, at different iteration numbers.

Results, by varying the number of iterations, for the improved Max-Log-MAP turbo decoder with the turbo interleaver 2 are depicted in Figure 6, for BPSK (on the left) and 16-QAM (on the right) modulations. For the BPSK modulation after the twentieth iteration the total gain compared to the first iteration is roughly 7.6 dB, at a BER = 10^{-3} . However, we note that most of the gain is obtained within the first three iterations. In particular, the second iteration allows a gain of 5.8 dB over the first, while the third gives an extra gain of 1 dB over the second. With the 16-QAM modulation the total gain from the first to the twentieth iteration is even greater and it is equal to 12.2 dB.

Finally, in Figure 7 we report the performance of the improved Max-Log-MAP decoder with 10 iterations by varying the turbo interleaver's length, for BPSK (on the left) and 16-QAM (on the right) modulations. As a comparison, we have also included the performance obtained with an un-coded HomePlug AV system over the same scenario. We observe

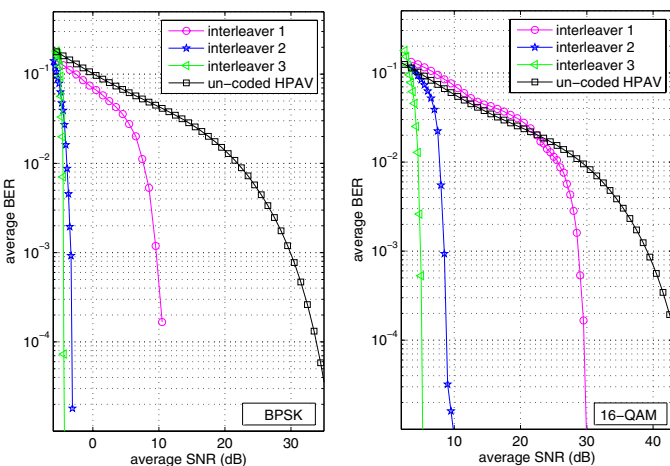


Fig. 7. Average BER versus average SNR, over a power-line channel: BPSK on the left and 16-QAM on the right. Performance of the improved Max-Log-MAP algorithm with different turbo interleavers and 10 iterations.

that, with all the interleavers, the turbo coded system provides a massive improvement with respect to the un-coded case. For instance, at a BER = 10^{-3} the turbo interleaver 1 gains roughly 20.3 dB with respect to the un-coded curve for the BPSK modulation, while 10.4 dB for the 16-QAM modulation. As in the AWGN channel, the maximum improvement is obtained with interleaver 3, which offers a further gain of 14 dB compared to interleaver 1 for the BPSK modulation, while 23.8 dB for the 16-QAM modulation.

VI. CONCLUSIONS

In this paper new results have been reported showing the effectiveness of the iterative turbo decoder of the HomePlug AV system over AWGN and power-line channels. In particular, results have shown that an improved Max-Log-MAP decoder performs very close to the more complex MAP decoder. Moreover, few iterations of the turbo decoding process appeared to give a massive gain in performance within the considered environment. Hence, implementations, where the number of the iterations is limited, could be attractive for a reduction of computational complexity and a marginal loss in performance.

Finally, a possible extension to this contribution may be to derive equivalent results, where bit-loading over the different OFDM sub-carriers is also introduced in the HomePlug AV system.

REFERENCES

- [1] HomePlug PowerLine Alliance, "HomePlug AV baseline specification," Version 1.0.00, Dec. 2005.
- [2] E. Biglieri, "Coding and modulation for a horrible channel," *IEEE Comm. Mag.*, vol. 41, pp. 92-98, May 2003.
- [3] C. Berrou, A. Glavieux and P. Thitimajshima, "Near Shannon limit error-correcting coding and decoding: Turbo-codes. 1," *IEEE ICC 1993*, pp. 1064-1070, May 1993.
- [4] A.G. Amat, S. Benedetto, G. Montorsi, D. Vogrig, A. Neviani and A. Gerosa, "An analog turbo decoder for the rate-1/3, 40 bit, UMTS turbo code," *IEEE ICC 2005*, pp. 663-667, May 2005.
- [5] D. Divsalar and F. Pollara, "Turbo codes for deep-space communications," *TDA progress report, Jet propulsion laboratory, California institute of technology*, pp. 42-120, Feb. 1995.
- [6] "HomePlug AV white paper," <http://www.homeplug.org>
- [7] K. H. Afkhamie, S. Katar, L. Yonge and R. Newman, "An overview of the upcoming HomePlug AV standard," *ISPLC 2005*, pp. 400-404, April 2005.
- [8] J. Vogt and A. Finger, "Improving the max-log MAP turbo decoder," *IEEE Elect. Lett.*, vol. 36, pp. 1937-1938, Nov. 2000.
- [9] A. J. Viterbi, "An intuitive justification and a simplified implementation of the MAP decoder for convolutional codes," *IEEE Journal on Select. Areas in Comm.*, vol. 16, pp. 260-264, Feb. 1998.
- [10] L. R. Bahl, J. Cocke, F. Jelinek and J. Raviv, "Optimal decoding of linear codes for minimizing symbol error rate," *IEEE Trans. on Inform. Theory*, vol. 20, pp. 284-287, March 1974.
- [11] S. Morosi, E. Del Re, R. Fantacci and D. Forasacchi, "Turbo-coding and bit-loading algorithms for a HomePlug-like DMT PLC system," *IEEE ISPLC 2006*, pp. 227-231, March 2006.
- [12] F. Tosato and P. Bisaglia, "Simplified soft-output demapper for binary interleaved COFDM with application to HIPERLAN/2," *IEEE ICC 2002*, pp. 664-668, May 2002.
- [13] H. Phillips, "Modeling of powerline communication channels," *ISPLC 1996*, pp. 724-728, Nov. 1996.
- [14] M. Zimmermann and K. Dostert, "Analysis and modeling of impulsive noise in broad-band powerline communications," *IEEE Trans. on Elect. Comp.*, vol. 44, pp. 249-258, Feb. 2002.
- [15] R. Hormis, I. Berenguer and X. Wang, "A simple baseband transmission scheme for power line channels," *IEEE Journal on Select. Areas in Comm.*, vol. 24, pp. 1351-1363, July 2006.